Particle Nucleation during Microemulsion Polymerization of Methyl Methacrylate

François Bléger,[†,‡] A. Kamalakara Murthy,[†,§] Fernand Pla,[‡] and Eric W. Kaler*,[†]

Center for Molecular and Engineering Thermodynamics, Department of Chemical Engineering, University of Delaware, Newark, Delaware 19716, Laboratoire des Sciences du Génie Chimique, UPR 6811 CNRS, Ecole Nationale Supérieure des Industries Chimiques, INPL, B.P. 451, F54001 Nancy Cedex, France, and KAI Science and Technology, Inc., P.O. Box 4691, Lancaster, Pennsylvania 17604-4691

Received March 8, 1993; Revised Manuscript Received January 25, 1994[•]

ABSTRACT: The evolution of the reaction conversion and particle size distribution during the microemulsion polymerization of methyl methacrylate (MMA) is used to determine the particle nucleation mechanisms. A pseudo-3-component oil-in-water microemulsion is formed with water, MMA, and a mixture of dodecyltrimethylammonium bromide (DTAB) and diodecyldimethylammonium bromide (DDAB) in a 3:1 weight ratio as surfactant. Polymerization is initiated with either an oil-soluble or a water-soluble initiator and conversion followed either by measurement of the unpolymerized monomer concentration in samples taken during the reaction or by direct on-line densimetry. A two-stage process is observed. The first stage, described by a very slow increase in conversion, is attributed mainly to homogeneous nucleation, and the second stage, characterized by a much higher rate of conversion, involves continuous nucleation and is governed mainly by a micellar-entry mechanism.

Introduction

Emulsions and microemulsions are both mixtures of oil, water, and surfactant. Emulsions are kinetically stable but thermodynamically unstable. They are turbid and contain large (1–10 μm) monomer droplets and swollen micelles (2–5 nm). Microemulsions, on the other hand, are thermodynamically stable and contain small (2–10 nm) droplets or swollen micelles. Microemulsions appear transparent or translucent, and their formation, phase behavior, and microstructure have been investigated extensively.[1] Microemulsions are usually formed with larger ratios of surfactant to monomer than are typical in emulsion recipes.

The unique physical properties of microemulsions have led to the development of polymerization of organic monomers in microemulsion systems, with the primary goal of producing stable latexes with particle sizes close to those of the parent microemulsion droplets. The microlatexes thus obtained are bluish colored and are either translucent or turbid. The sizes of particles produced so far are larger than the size of the initial microemulsion droplets.[2]

Several features of the mechanism of microemulsion polymerization are unresolved, including the key problem of particle nucleation and growth. This question has been addressed extensively by Candau and co-workers[3,4] in the case of water-in-oil microemulsions, with the main conclusion that nucleation is continuous throughout the polymerization. The mechanism of oil-in-water (o/w) polymerization has been less studied. Early work on styrene o/w microemulsion polymerization by Guo et al.[5] and Pérez-Luna et al.[6] assumed that the nucleation occurs in the microemulsion droplets and that nucleation was limited to a first interval that lasts up to *ca.* 20% conversion. After reexamination of the same system, Guo et al.[7] postulated that in fact particle nucleation is continuous. They confirmed that the main locus of particle nucleation is the microemulsion droplets, although homogeneous nucleation and coagulation during polymerization were not completely ruled out.

The nucleation process in emulsion polymerization is much better understood and may provide clues about the microemulsion mechanism. Early studies of emulsion polymerization of styrene showed that latex particles were nucleated by a micellar-entry mechanism in which free radicals, produced by decomposition of the initiator, enter micelles swollen by monomer.[8] Later, study of emulsion polymerization of the more water-soluble monomer methyl methacrylate led to the discovery of the homogeneous nucleation mechanism.[9] During homogeneous nucleation, a water-soluble free radical reacts with several monomers in the water phase, thus producing growing polymer chains that ultimately precipitate out of the water to form latex particles. In addition, Feeney et al.[10] have proposed that new particles may also form as the result of coagulation of several unstable particles. All or part of the above mechanisms may be active in any emulsion system, depending chiefly on the water solubility of the monomer and on the ratio of monomer to surfactant.

Since all the species acting in these nucleation processes are present in a microemulsion, any or all of these mechanisms could be important during microemulsion polymerization. In the micellar-entry mechanism, microemulsion droplets play the role of monomer-swollen micelles.

The main object of this study is to determine the particle nucleation mechanism(s) in the microemulsion polymerization of methyl methacrylate. This monomer is relatively soluble in water and so should be susceptible to homogeneous nucleation. Moreover, the relatively low stability of poly(methyl methacrylate) particles[11,12] could promote coagulation nucleation. Particle nucleation is very difficult to observe. Here, the measurement of monomer to polymer conversion was made using high-performance liquid chromatography (HPLC), which measures residual monomer content and on-line densimetry, which provides a continuous and precise reading of the conversion. The evolution of particle sizes was recorded on transmission electron micrographs of samples quenched during the reaction.

† Center for Molecular and Engineering Thermodynamics.
‡ Laboratoire des Sciences du Génie Chimique.
§ KAI Science and Technology.
• Abstract published in *Advance ACS Abstracts*, March 15, 1994.

0024-9297/94/2227-2559$04.50/0

We used a mixture of two cationic surfactants, dodecyltrimethylammonium bromide (DTAB), a single-tailed surfactant, and its double-tailed analog didodecyldimethylammonium bromide (DDAB). DTAB/H_2O/MMA mixtures produce oil-in-water microemulsions, while DDAB/H_2O/MMA mixtures produce water-in-oil microemulsions. Combinations of DTAB and DDAB with water and MMA open a bridge between the water-rich and the oil-rich corners of the phase diagram. The large microemulsion area thus created offers a rich structural morphology of oil-in-water, bicontinuous, and water-in-oil microemulsions.

Experimental Section

Reagent-grade methyl methacrylate (Scientific Polymer Products 99%) inhibited with 10 ppm hydroquinone monomethyl ether was passed over a DHR-4 column (Scientific Polymer Products) to remove the inhibitor prior to polymerization. Didodecyldimethylammonium bromide (DDAB) (Tokyo Kasei 98+%) and *n*-dodecyltrimethylammonium bromide (DTAB) (Tokyo Kasei 99+%) were used without further purification. Azobis(isobutyronitrile) from DuPont, potassium persulfate from J. T. Baker, and V50 (2,2'-azobis(2-amidinopropane)dihydrochloride) from Wako were used as received. The water was distilled, deionized, and filtered. Hydroquinone was purchased from Aldrich. Acetonitrile and methanol were HPLC grade from Fisher Scientific.

All the experiments were carried out with a mixture of the two surfactants, DTAB and DDAB, at a fixed weight ratio of 3:1. The single-phase microemulsion regions at 25 and 60 °C were determined visually by preparing samples by weight. For phase behavior observations, the inhibitor was not removed from the methyl methacrylate. Samples were observed between crossed sheets of polarizing plastic to check for static or streaming birefringence.

All the microemulsions were polymerized for 2 h at 60 °C. The polymerized microemulsion contained by weight 90% water, 5% methyl methacrylate, 3.75% DTAB, and 1.25% DDAB. Either the water-soluble initiator V50 or the oil-soluble initiator AIBN was used. The surfactants and degassed water were mixed 12 h before polymerization, and then this mixture and the monomer were purged overnight to remove dissolved oxygen before being mixed together to form the microemulsion. Depending on the kinetic measurements and sample analysis required, either a 100-mL or a 2-L reactor was used. The reactor size and initiator type and concentration are given for each run in Table 1.

Runs R1–R10 were performed in a 100-mL glass reactor equipped with reflux, an inlet to blanket the reacting medium with argon, and an outlet for sampling. For polymerization initiated with V50, the prepared microemulsion was loaded into the reactor, heated to 60 °C, and initiated by injecting a concentrated aqueous solution of V50. For AIBN initiation, AIBN was dissolved in all or part of the monomer, which was then added to the prepared microemulsion and heated to 60 °C.

Table 1. Initiator Type and Concentration and Final Latex Particle Diameter

run no.	initiator type	initiator concn wt %/ monomer	initiator concn mol/mol of monomer (×10³)	final particle diameter (nm)
R1	V50	2	7.34	60
R2	V50	1	3.67	54
R3	V50	0.5	1.83	60
R4	V50	0.2	0.734	60
R5	V50	0.1	0.367	62
R6	AIBN	2	12.2	60
R7	AIBN	1	6.10	60
R8	AIBN	0.5	3.05	62
R9	AIBN	0.2	1.22	60
R10	AIBN	0.1	0.61	62
R11[a]	V50	0.5	1.83	52

[a] All reactions were run in 100-mL glass reactors except for R11, which was carried out in a 2-L reactor. See text.

In both cases, the mixture was continually stirred under a positive pressure of argon. Samples were taken before, during, and after polymerization in order to follow the conversion and the particle size. Reacting samples were quenched by hydroquinone and put in an ice bath.

Polymerization run R11 was carried out under nitrogen in a 2-L jacketed reactor equipped with reflux and an on-line densimeter (Anton-Paar, Model DPR 412 YE) to measure the conversion (see below). A sampling loop circulated the reacting medium through the densimeter cell.

Except for run R11, the conversion was measured by analysis of residual monomer by HPLC as follows. A known amount of sample was precipitated in a known amount of methanol and centrifuged to separate the polymer. Separate experiments showed all monomer partitioned in the upper phase. Part of the upper phase was then diluted with water prior to injection into a Hewlett-Packard Model 1090 HPLC equipped with a 20-μL injection loop and a refractive index detector. The column was 150-mm long and 4.6-mm in diameter and was packed with 5-μm Nucleosil C18 particles. The mobile phase was a mixture of 40% water and 60% acetonitrile flowing at 1 mL/min.

For run R11, the conversion was determined by densimetry. The measured values of the reacting microemulsion density were corrected to the setpoint of the reaction temperature using the temperature coefficient of expansion of the measuring tube and an average temperature coefficient of the density weighted according to the (conversion-dependent) volume fractions of the components of the microemulsion. The volume of the dispersed phase was considered to contract linearly with conversion, i.e., $V = V_0\,(1 + \epsilon X_{MMA})$, where $\epsilon = (\rho_0/\rho_1) - 1$, ρ_0 and ρ_1 are the densities of the dispersion at the beginning and at the end of the reaction, and V_0 and V are the volume of microemulsion at the beginning and during the polymerization respectively. The fractional monomer conversion, X_{MMA}, which is usually defined on the basis of the number of moles, can be calculated for batch polymerization as

$$X_{MMA} = \frac{n_0 - n}{n_0} = \frac{V_0 - V}{V_0 - V_1} \frac{\rho(t) - \rho_0}{\rho_1 - \rho_0} \frac{\rho_1}{\rho(t)}$$

where n_0 and n are the number of moles of monomer at the beginning of the polymerization and during the polymerization, respectively. $\rho(t)$ is the measured density of the dispersion during the reaction, and V_1 is the final volume of latex.

The accuracy of the density measurements is 10^{-4} g/cm³. Thus, the expected precision of the conversion measurement is *ca.* ±1%. The densimeter reads the density once per second, and these values were averaged to yield one point per minute. The average residence time in the sampling loop was less than 1 min.

The particle size was analyzed by quasielastic light scattering. Latexes were diluted between 100 and 200 times to minimize particle–particle interactions and then filtered through Gelman 0.45-μm acrodisc 13 CR PTFE filters to eliminate dust. The quasielastic light-scattering measurements were made with equipment previously described.[13] Intensity correlation data were analyzed by the method of cumulants to provide the average decay rate, $\langle\Gamma\rangle = 2q^2D$ where D is the diffusion coefficient and q is the scattering vector [$q = (4\pi n/\lambda_0)\sin(\theta/2)$ where θ is the scattering angle, n is the index of refraction, and λ_0 is the wavelength of the light in vacuum]. The measured diffusion coefficients were represented in terms of apparent radii using the Stokes–Einstein equation and assuming the solvent has the viscosity of water.

The evolution of the particle size distribution for run R11 was measured directly from transmission electron micrographs (Zeiss T.E.M.). A drop of latex sample diluted one hundred times was deposited on a grid, a drop of a 2% solution of the negative stain phosphotungstic acid was added, and the grid was dried overnight. At least 400 particles per sample were counted to estimate the particle size distribution. No size standards were used, and reported sizes were calculated from the instrument magnification. The sizes thus have a precision of no better than ca. ±10%.

For molecular weight determination, a fraction of latex was precipitated in hot methanol and thoroughly washed with hot methanol and hot water in order to remove all of the surfactants.

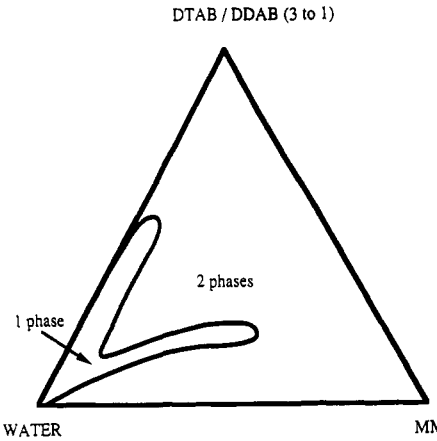

Figure 1. Pseudoternary phase diagram of the system DTAB and DDAB/methyl methacrylate/water at 25 °C.

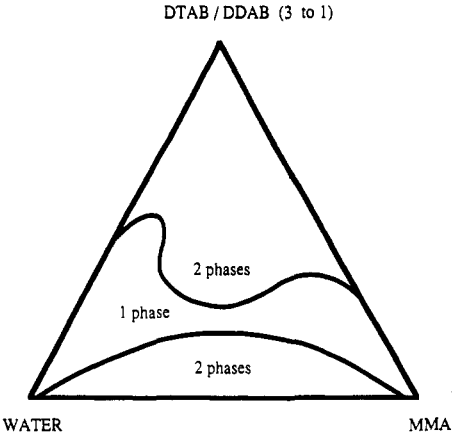

Figure 2. Pseudoternary phase diagram of the system DTAB and DDAB/methyl methacrylate/water at 60 °C.

The polymer was then dried in a vacuum oven at 50 °C for 24 h. At least 1 g of dried polymer was used.

Weight and number average molecular weights (M_w and M_n) as well as the molecular weight distribution (MWD) were determined by on-line size exclusion chromatography (SEC) and low angle laser light scattering (LALLS). The chromatographic equipment includes a Waters MS10 solvent-delivery system, a pulsation attenuator, a U6K injector, a series of two linear Ultrastyragel columns (Waters) in a thermostated oven, a Waters R410 differential refractometer, and a Chromatix KMX-6 LALLS detector equipped with a 10-μL cell. Chromatix measurements were made using a wavelength of 632.8 nm and instrumental parameters set to 6–7° annulus and 0.15 field stop. Elutions were performed with tetrahydrofuran (THF)-stabilized with 2,6-di-*tert*-butyl-4-methylphenol with a column temperature of 40 °C and a detector temperature of 35 °C. The flow rate was 1 cm³/min, the injected volume was 25 μL, and the concentration of the injected solution was about 5 mg/cm³. The solvent and solutions were filtered through a 0.2-μm Millipore membrane to remove dust.

The refractive index increments were taken as 0.091 mL/g for methyl methacrylate in THF at a wavelength of 633 nm.[14] The refractive index of the solvent (n_0 = 1.405) was determined at λ = 632.8 nm and T = 35 °C using an Abbe refractometer and the second virial coefficient ($A_2 = 4 \times 10^{-4}$ mol·ml·g^{-2}) was obtained from static light scattering measurements.

The number of polymer chains per particle was calculated using the mean particle radius and the average molecular weight. The apparent polydispersity of the particle size distribution as determined by QLS and observation of the micrographs makes this calculation somewhat untrustworthy, and this number is not very accurate.

Results

Phase Diagram. The pseudo-ternary phase diagram of cationic amphiphiles/methyl methacrylate/water was determined at 25 and 60 °C in order to find the extent of the microemulsion phase (Figures 1 and 2). At 25 °C, methyl methacrylate is sparingly soluble in water (1.59% at 20 °C).[15] As surfactant is added, the mutual solubility increases until the mixture forms a transparent single-phase microemulsion. This region has the shape of two fingers, one poor in monomer and containing up to 50% surfactants and the other less rich in amphiphile but extending up to 45% monomer. Outside the one-phase region we observed only two-phase samples.

At 60 °C, the one-phase region increases to form a bridge between the water-rich and the oil-rich corners (Figure 2). This phase probably contains an oil-in-water microemulsion on the water-rich side, a water-in-oil microemulsion on the oil-rich side, and a bicontinuous microemulsion in between.[16,17] The one-phase region observed at 25 °C is approximately contained in the one observed at 60 °C.

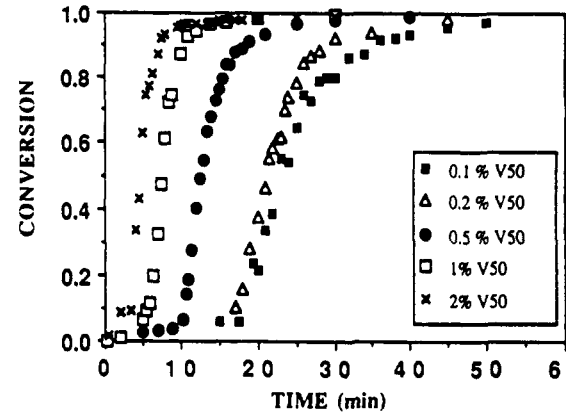

Figure 3. Evolution of the conversion versus time for five different concentrations of V50 as measured by HPLC.

Kinetic Study. The kinetic study was carried out on a formulation chosen for its stability and its relatively low surfactant to monomer ratio. Increasing the monomer concentration above 5% dramatically decreases the stability of the final latex, and for monomer concentrations above 10%, the polymer precipitates. The most studied water-soluble initiator for this type of polymerization is potassium persulfate, and some preliminary experiments were carried out with this product. However, the microemulsion at 25 °C became turbid when potassium persulfate was introduced, suggesting an interaction between the negatively charged potassium persulfate and the cationic surfactant. Therefore, potassium persulfate was discarded in favor of V50, a cationic initiator.

For polymerizations initiated with V50, the evolution of conversion versus time for five different initiator concentrations is shown in Figure 3. The final conversion is close to 100% and decreases as the concentration of V50 drops. After an initial slow period of conversion, which shrinks with increasing initiator concentration, the conversion reached 90% in 8 min for the largest amount of V50 (run R1) and 20 min for the smallest one (R5). The change in reaction rate coincides with the appearance of a bluish tint in the polymerizing solution.

Similar experiments have been conducted with AIBN. The evolution of conversion versus time for polymerizations initiated by different AIBN concentrations (Figure 4) exhibits the same trends as those observed when V50 was used. The first slow stage is longer with decreasing initiator concentration and lasts up to 60 min for run R10. The final conversion reached after 2 h of reaction is above 90% but is smaller than the final conversion produced with V50.

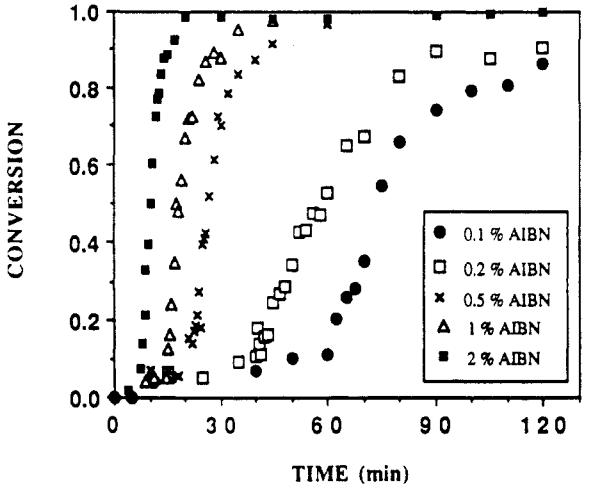

Figure 4. Evolution of the conversion versus time for five different concentrations of AIBN as measured by HPLC.

Table 2. Average Polymer Molecular Weights and Polydispersities and the Number of Polymer Chains per Particle (Based on the Radius Measured by QLS)

run	M_n ($\times 10^{-6}$)	M_w ($\times 10^{-6}$)	M_z ($\times 10^{-6}$)	I_n ($= M_w/M_n$)	I_w ($= M_z/M_w$)	no. of chains per particle
R1	1.34	1.59	1.84	1.18	1.16	60
R5	1.82	2.16	2.44	1.19	1.13	53
R6	4.00	4.50	4.72	1.12	1.05	19
R10	4.14	4.63	5.02	1.12	1.09	20

Final particle size as a function of initiator concentration for both V50 and AIBN is given in Table 1. The final latex particle size does not depend on initiator concentration or type.

Weight-average, number-average, and z-average molecular weights (M_n, M_w and M_z respectively) and their polydispersity indices ($I_n = M_w/M_n$) and ($I_w = M_z/M_w$) are given in Table 2 for runs R1, R5, R6, and R10. The molecular weights are very high and are close to the exclusion limit of the column, but the chromatographs are well resolved and symmetric. Molecular weights obtained by AIBN initiation are twice those obtained using V50. In every case, the polydispersity is low ($1.095 < I_n < 1.19$ and $1.075 < I_w < 1.16$). The molecular weight dependence on initiator concentration is greater for V50 than for AIBN. The calculated number of polymer chains per particle is approximately 20–60, with a higher number of chains produced using AIBN.

In order to confirm the two-stage evolution of the reaction, the densimeter was employed for run R11 to give a continuous reading of the conversion with greater precision than the HPLC method. The evolution of conversion with time (Figure 5) confirms the two-stage process observed previously (R1–R10). For this concentration of V50, the first stage lasts for 5 min and the conversion reaches 8%. Subsequently, the rate increases markedly. The particle size distribution at the transition between these two rate regimes is fairly sharp, with a number average diameter of 18.4 nm (Table 3). At 25% conversion, the size distribution shifts towards higher sizes, while the width of the distribution increases (Figure 6). These distributions were determined from the TEM photographs shown in Figure 7. At higher conversions, the polydispersity of the particle sizes increases slightly while the mean diameter remains constant. As is usually observed, the size determined by microscopy is smaller than the apparent radius measured by QLS (Table 3).

The numbers of polymer particles in each category of the distribution of particle size are summed to give the total number of particles per mL of latex (Table 3). The total number of particles increases with conversion, doubling over the course of the polymerization.

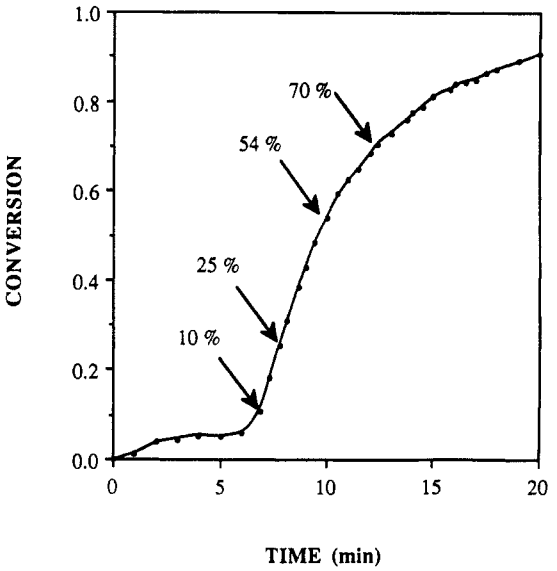

Figure 5. Evolution of the conversion versus time for run R11 measured by on-line densimetry.

Discussion

It is important to establish that part of the kinetic results are not artifacts arising from any residual inhibitors such as oxygen or hydroquinone. In these microemulsions oxygen content does not increase during the reaction since no oxygen is produced by the decomposition of the initiators used.[18] Samples are also extensively purged before the reaction begins. As seen from Figures 3–5, the conversion of monomer to polymer is faster after an initial period of "retardation", which, for the slower runs, can be decomposed into an induction period, where there is no conversion, and a "slow regime" where the conversion picks up and finally reaches 5–10%. According to studies of the emulsion polymerization of styrene,[19] the induction period caused by oxygen is inversely proportional to the amount of initiator, I. Thus the product of [I] and the induction time should be a constant for this process. The length of the period of retardation is compared to the initiator concentration in Table 4. The calculated product of the duration of the retardation period and [I] increases with increasing initiator concentration, thus showing that at most only part of the induction period can be attributed to oxygen. Furthermore, the inhibitor constant of oxygen is large (33 000) for methyl methacrylate (at 50 °C) so oxygen should only inhibit and not retard the polymerization.[20] Thus, if oxygen is active, no conversion should be seen during an induction time. Evidently, the bulk of the observed slow initial regime is due to other mechanism(s).

Before addressing the possible mechanisms active in microemulsion polymerization, it is useful to review some of the differing aspects of the emulsion polymerization of methyl methacrylate and styrene. MMA is moderately soluble in water and so is prone to polymerization by homogeneous nucleation. The critical degree of polymerization before precipitation as a polymer particle is roughly 65 for MMA, while it is about 8 for styrene.[21] Pioneering work of Yeliseyeva[22] on the polymerization of polar monomers addressed some of the effects of polarity on surfactant adsorption and the kinetics of emulsion polymerization of polar monomers. In emulsion polymerization, the stability of particles and their growth by

Table 3. Particle Diameter of Samples fron Run R11 As Measured by TEM and QLS and the Number of Particles per Volume

convn (%)	no.-av. diameter D_n (nm) by TEM	wt-av. diameter D_w (nm) by TEM	polydispersity index $I_n = D_w/D_n$	app diameter QLS (nm)	no. of particles per mL of latex ($\times 10^{15}$)
10	18.4	20.5	1.11		2.44
25	26.3	29.1	1.11		2.10
43	26.5	31.5	1.19	42	3.20
54	25.3	30.2	1.19	49	4.64
70	27.1	31.5	1.17	49	5.05

Table 4. Duration of the Retardation Period for Different Concentrations of V50 and AIBN and the Product of the Retardation Period and the Initiator Concentration

AIBN concn (wt %/MMA)	retardation with AIBN (min)	concn × retardation (for AIBN)	V50 concn (wt %/MMA)	retardation with V50 (min)	concn × retardation (for V50)
2.00	6	12.00	2.00	3	6.00
1.00	15	15.00	1.00	6	6.00
0.50	22	11.00	0.50	10	5.00
0.20	40	8.00	0.20	17	3.40
0.10	60	6.00	0.10	18	1.80

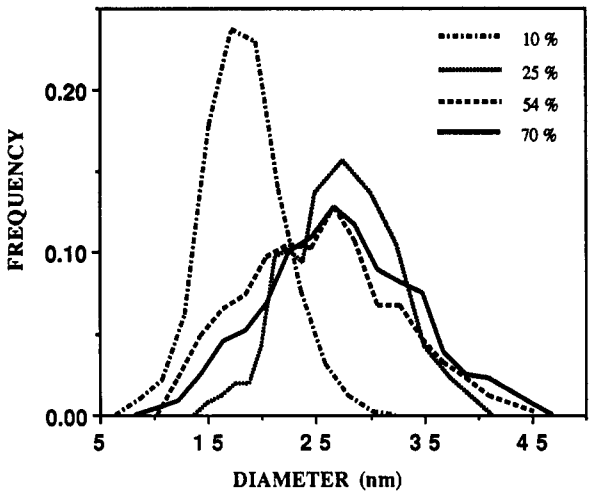

Figure 6. Evolution of the particle size distribution with conversion for run R11. Distributions measured from the TEM micrographs of Figure 7.

monomer swelling are greatly influenced by the polarity of the water–monomer and water–polymer interfaces.[23,24] The adsorption of surfactants on the final latex particles is also different and suggests, not surprisingly, that the MMA surface is more polar. Polymers of styrene and MMA have also been made via surfactant-free emulsion polymerization (with persulfate initiation).[25–27] In this process, the size and surface charge density of the primary particles produced from styrene oligomers are similar to those of sodium dodecyl sulfate micelles,[27] while in contrast MMA particles have high molecular weights and low surface charge densities. During the growth period, the styrene particles are more stable than MMA particles, and stabilization of MMA particles by surfactant adsorption is hindered by the polar nature of the MMA polymer surface. Although these conclusions are drawn from emulsion polymerization studies, we expect similar influences of the monomer properties of the kinetics of microemulsion polymerization because the water–monomer and water–polymer interface polarity is dictated only by the monomer properties.

There are three possible loci for polymerization in emulsions, (1) monomer-swollen micelles, (2) the aqueous phase, and (3) the monomer droplets, but only the first two are favored.[28] In microemulsion polymerization only the first two loci, microemulsion droplets and the aqueous domain, are available for particle nucleation. In both emulsion and microemulsion polymerization, the relative importance of each mechanism depends on the emulsion and the polymerization conditions. Surfactant concentrations above the critical micelle concentration (CMC) and the presence of a hydrophobic monomer favor the micelle-entry nucleation process. In microemulsions of polar monomers, both micelle-entry and homogeneous nucleation can proceed.[29,30]

Given the high water solubility of methyl methacrylate and the surfactant concentrations employed in our polymerization studies, both homogeneous and micelle-entry nucleation mechanisms are likely to be active. In particular, the evidence shows that a slow rate regime is observed up to ca. 10% and is followed by a sharp increase in rate (Figure 5). At the time the rate increases, the particle size distribution broadens (Figure 6). We propose that these shifts in the rate and the particle size distribution correspond to a change from homogeneous nucleation in the early stages to predominantly a micelle-entry mechanism as the reaction proceeds.[22]

Initial retardation periods have been observed by other authors for styrene (Figure 3 of Feng and Ng[31] or Figures 2 and 4 of Pérez-Luna et al.[6]), and the duration of the retardation periods for styrene and methyl methacrylate can be compared. For styrene microemulsion polymerization[6] with an AIBN concentration of 6.4×10^{-4} mol/mol of monomer, the first period lasts 25 min. In the present study with MMA, with the same concentration of AIBN and the same degassing precautions, the first period lasts 60 min (run R10). This difference is consistent with a homogeneous nucleation mechanism because for styrene, where the critical polymer radical contains eight monomers, the homogeneous nucleation period is shorter than for methyl methacrylate, where the critical polymer radical contains 65 units.[22]

In the Smith–Ewart theory of emulsion polymerization,[28] particle generation is assumed to cease with the depletion of surfactant micelles. Given the large excess of surfactant, this situation is never met in microemulsion polymerization and particles continue to be generated during the course of polymerization. The increase in total number of particles in the latex with conversion (Table 3) provides evidence for this continuous generation. The presence of continuous nucleation has been inferred by others.[3,4,7,32,33]

In the MMA microemulsions of interest here, in which there is apparently homogeneous nucleation and the polymer is soluble in the monomer, there will be high probability of active growing chains coalescing with monomer-swollen polymer particles, resulting in polymer particles containing more than one polymer chain. The present polymer particles average many more than two chains per particle (Table 2).

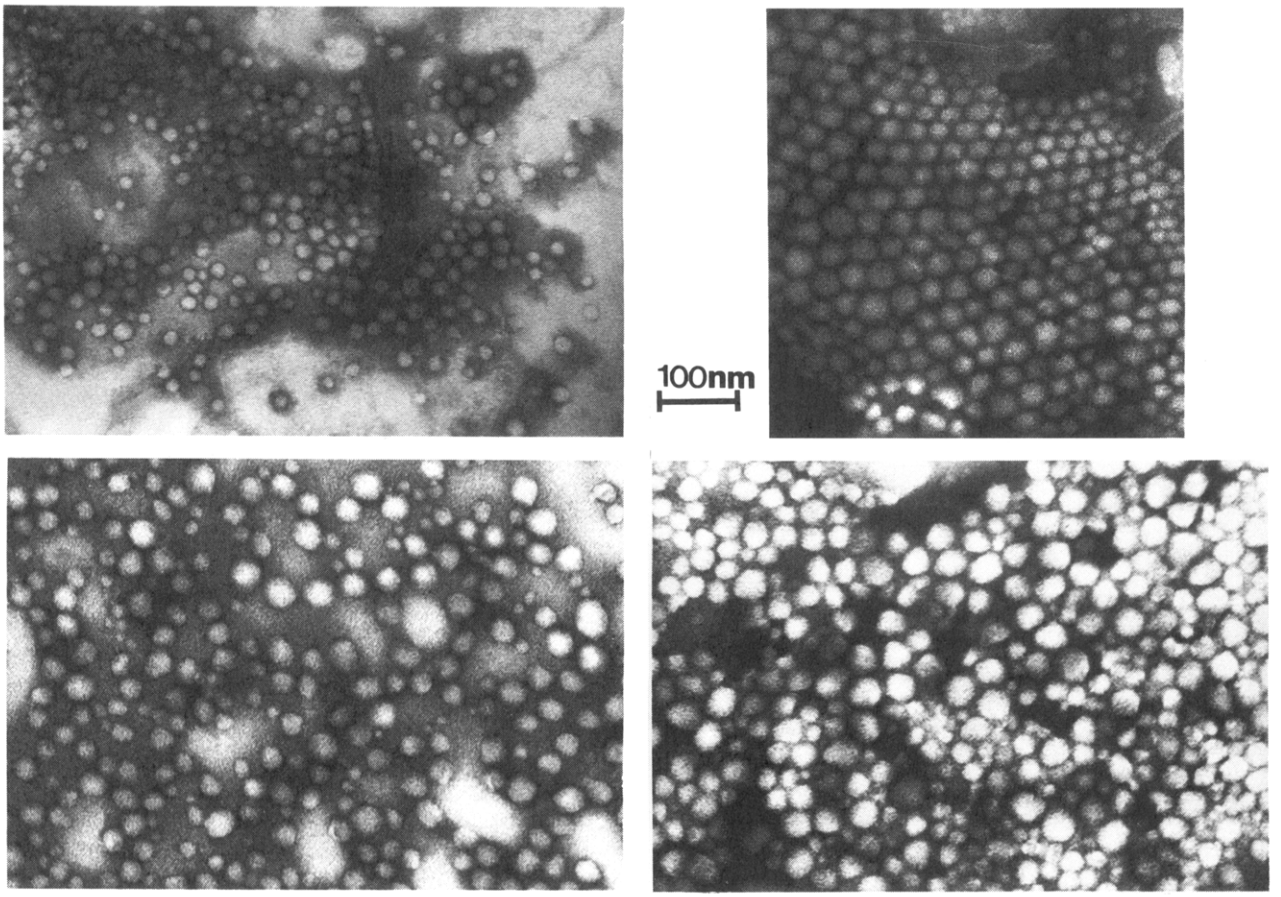

Figure 7. Transmission electron micrographs of polymer particles produced during run R11 at different conversions (see Figure 6): (top left) 10% conversion, (top right) 25%, (bottom left) 54%, (bottom right) 70% (magnification: ×85000).

In summary, the microemulsion polymerization of MMA in this system, when initiated with V50, begins with homogeneous nucleation and continues via a micelle-entry nucleation mechanism. The evolution of the particle size distribution with conversion published here is strikingly similar to the one published by Guo et al.[7] for styrene, so this two-stage process may be a general feature of oil-in-water microemulsion polymerization.

We have also investigated the locus of particle nucleation with an oil-soluble initiator and find similar behaviors. For both V50- and AIBN-initiated polymerizations, the major trend of a two-stage evolution of the conversion versus reaction time is recorded (see, for example, R3 and R8 in Figures 3 and 4). V50 produces free radicals at 60 °C 30 times faster than does AIBN.[34] Thus, results produced at equal rates of free-radical production should be used to compare the length of each stage (R5 and R6), but surprisingly the first rate regime is longer with V50 (Table 4). This is a consequence of the fact that free radicals produced by the decomposition of V50 have the same charge as the microemulsion droplets. The repulsion between these two species increases the probability of reaction between a cationic free radical and dissolved monomer, thus promoting homogeneous nucleation rather than micellar entry. This explanation is consistent with the hypothesis that homogeneous nucleation is predominant during the first stage of the reaction.

AIBN is mainly dissolved in the oil, and homogeneous nucleation is less likely than with V50. Moreover, homogeneous nucleation yields primary particles that are prone to limited flocculation. Therefore, the longer regime of homogeneous nucleation seen with V50 should yield a higher number of polymer chains per particle at the end of the polymerization, as is observed (particles produced using V50 (R5) contain three times more chains than particles produced using AIBN (R6), Table 2). No differences between R5 and R6 are shown in the second stage of reaction. Final particle size is independent of initiator type and concentration (Table 1), as previously observed.[35,36]

Similar experiments were conducted to study the kinetics of styrene microemulsion polymerization,[5,6] and no major differences in mechanism were observed between polymerizations initiated by water-soluble or oil-soluble initiators.

For emulsion polymerization, numerous studies comparing oil- and water-soluble initiators have been conducted, most of them showing an unexpected similarity of behavior. Water-soluble initiators produce radicals that appear in particles one at a time. The similarity of behavior is believed to depend on the ability of oil-soluble initiators to yield single radicals. Two hypotheses have been proposed to explain the origin of single radicals in oil-soluble-initiated polymerization, namely that either the very small portion of the oil-soluble radicals dissolved in the water phase is responsible for the single radicals[37,38] or there is desorption of free-radical species from the swollen micelles.[39,40]

In our system, AIBN is mainly located in the microemulsion droplets. At the beginning of the polymerization, because of the very small size of the droplets, the probability of fast recombination of the two oligomeric radicals produced by AIBN decomposition is high. Thus, very few particles will be nucleated by the simultaneous growth of these two oligomeric radicals, and radicals from the water phase will play a major role. Regardless of how free radicals are produced in the continuous phase of the microemulsion, their presence explains the observed

similarity between V50 and AIBN initiated polymerization. Therefore, the two-stage process proposed for V50 initiation can be extended to describe AIBN initiation. Because of the small size of the particles it is unlikely that a "gel" effect is influencing the observed rates.[42]

Conclusion

Microemulsion polymerization of methyl methacrylate in a pseudoternary system follows a two-stage process. During the first part of the reaction, the global polymerization rate is slow and nucleation of latex particles occurs mainly in the water phase, regardless of the type of initiator used. The second stage of the polymerization has a much higher rate of polymerization. The nucleation of latex particles is continuous throughout the reaction and occurs mainly in the microemulsion droplets.

A similar two-stage process is observed during the oil-in-water microemulsion polymerization of styrene solubilized by various surfactant systems,[6,31] and the evolution of the particle size distributions with conversion are similar for styrene and MMA. This two-stage process may be a general feature of oil-in-water microemulsion polymerization.

Acknowledgment. We are very grateful to Dr. Jorge Puig for his guidance in the selection of the DTAB/DDAB surfactant mixture, and we thank Kate A. Marritt for her help with some of the experiments. We are also indebted to Robert Weiland and Dr. R. Wagner for their competent help with the electron microscopy experiments. Support of this work by the Société Française Hoechst is gratefully acknowledged.

References and Notes

(1) Langevin, D. *Adv. Colloid Interface Sci.* **1991**, *34*, 583.
(2) Friberg, S. E., Venable, R. L. In *Encyclopedia of Emulsion Technology*; Becher, P., Ed.; Marcel Dekker: New York, 1983, Vol. 1.
(3) Candau, F.; Leong, Y. S.; Fitch, J. R. *J. Polym. Sci., Polym. Chem. Ed.* **1985**, *23*, 193.
(4) Carver, M. T.; Hirsch, E.; Wittman, J. C.; Fitch, R. M.; Candau, F. *J. Phys. Chem.* **1989**, *93*, 4867.
(5) Guo, J. S.; El-Aasser, M. S.; Vanderhoff, J. W. *J. Polym. Sci., Polym. Chem. Ed.* **1989**, *27*, 691.
(6) Pefez-Luna, V. H.; Puig, J. E.; Castaño, V. M.; Rodríguez, B. E.; Murthy, A. K.; Kaler, E. W. *Langmuir* **1990**, *6*, 1040.
(7) Guo, J. S.; Sudol, E. D.; Vanderhoff, J. W.; El-Aasser, M. S. *J. Polym. Sci., Polym. Chem. Ed.* **1992**, *30*, 691.
(8) Harkins, W. D. *J. Am. Chem. Soc.* **1947**, *69*, 1428; *J. Polym. Sci.* **1947**, *5*, 217.
(9) Fitch, R. M.; Tsai, C. H. In *Polymer Colloids I*; Fitch, R. M., Ed.; Plenum: New York, 1971, p 73.
(10) Feeney, P. J.; Napper, D. H.; Gilbert, R. G. *Macromolecules* **1984**, *17*, 2520.
(11) Vijayendran, B. R. *J. Appl. Polym. Sci.* **1979**, *23*, 733.
(12) Paxton, T. R. *J. Colloid Interface Sci.* **1969**, *31*, 19.
(13) Chang, N. J. Ph.D. Thesis, University of Washington, **1986**.
(14) Brandrup, J.; Immergut, E. H. *Polymer Handbook*; John Wiley: New York, 1975.
(15) Min, K. W.; Ray, H. W. *J. Macromol. Sci. C Rev. Macromol. Chem.* **1974**, *11*, 177.
(16) Jahn, W.; Strey, R. *J. Phys. Chem.* **1988**, *92*, 2294.
(17) Scriven, L. E. *Nature* **1976**, *263*, 123.
(18) Goodwin, J. W.; Ottewill, R. H.; Pelton, R.; Vianello, G.; Yates, D. E. *Brit. Poly. J.* **1978**, *10*, 173.
(19) Bovey, F. A.; Kolthoff, I. M. *J. Am. Chem. Soc.* **1947**, *69*, 1501.
(20) Odian, G. *Principles of Polymerization*; John Wiley: New York, 1980; p 246. Hawkett, B. S.; Napper, D. H.; Gilbert, R. G. *J. Chem. Soc., Faraday. Trans. 1* **1980**, *76*, 1323.
(21) Fitch, R. M.; Tsai, C. H. In *Polymer Colloids I*; Fitch, R. M., Ed.; Plenum: New York, 1971; p 103.
(22) Yieliseyeva, V. I. In *Emulsion Polymerization*; Piirma, I., Ed.; Academic Press: New York, 1982; p 247.
(23) Zuikov, A. V.; Vesilenko, A. I. *Colloid J. USSR* **1976**, *37*, 584.
(24) Yeliseyeva, V. I.; Petrova, S. A. *Dok. Akad. Nauk. SSSR* **1972**, *202*, 45.
(25) Roe, C. P. *Ind. Eng. Chem.* **1968**, *60*, 20.
(26) Goodwin, J. W.; Hearn, J.; Ho, C. C.; Ottewill, R. H. *Colloid Polym. Sci.* **1974**, *252*, 464.
(27) Vanderhoff, J. W. *J. Polym. Sci., Polym. Symp.* **1985**, *72*, 161.
(28) Smith, W. V.; Ewart, R. H. *J. Chem. Phys.* **1948**, *16*, 592.
(29) Sutterlin, N.; Kurt, H. J.; Markert, G. *Makromol. Chem.* **1976**, *177*, 1549.
(30) Sutterlin, N. In *Polymer Colloids II*; Fitch, R. M., Ed.; Plenum: New York 1980.
(31) Feng, L.; Ng, K. Y. S. *Macromolecules* **1990**, *23*, 1048.
(32) Carver, M. T.; Candau, F.; Fitch, J. R. *J. Polym. Sci., Polym. Chem. Ed.* **1989**, *27*, 2179.
(33) Chamberlain, B. J.; Napper, D. H., Gilbert, R. G. *J. Chem. Soc., Faraday Trans. 1* **1982**, *78*, 691.
(34) Hammond, G. S.; Newman, R. C. *J. Am. Chem. Soc.* **1963**, *85*, 1501.
(35) Rodríguez-Guadarrama, L. A.; Mendizabal, E.; Puig, J. E.; Kaler, E. W. *J. Appl. Polym. Sci.* **1993**, *48*, 775.
(36) Antonietti, M.; Bremser, W.; Müshenborn, D.; Rosenauer, C.; Schupp, B. *Macromolecules* **1991**, *24*, 6636.
(37) Barton, J.; Kárpátyová, A. *Makromol. Chem.* **1987**, *188*, 693.
(38) Nomura, M.; Fujita, K. *Makromol. Chem., Rapid Commun.* **1989**, *10*, 581.
(39) Alduncin, J. A.; Forcada, J.; Barandiaran, M. J.; Asua, J. M. *J. Polym. Sci., Polym. Chem. Ed.* **1991**, *29*, 1265.
(40) Sudol, E. D.; El-Aasser, M. S.; Vanderhoff, J. W. *J. Polym. Sci., Polym. Chem. Ed.* **1986**, *24*, 3515.
(41) Brooks, B. W. *J. Polym. Sci., Polym. Chem. Ed.* **1991**, *29*, 1661.
(42) Russel, G. T.; Gilbert, R. G.; Napper, D. H. *Macromolecules* **1993**, *26*, 3538.